Eur Biophys J (2009) 38:807–812
DOI 10.1007/s00249-009-0501-6

ORIGINAL PAPER

Structured illumination microscopy of a living cell

Liisa M. Hirvonen · Kai Wicker · Ondrej Mandula · Rainer Heintzmann

Received: 26 February 2009 / Revised: 26 May 2009 / Accepted: 27 May 2009 / Published online: 18 June 2009

Abstract Due to diffraction, the resolution of imaging emitted light in a fluorescence microscope is limited to about 200 nm in the lateral direction. Resolution improvement by a factor of two can be achieved using structured illumination, where a fine grating is projected onto the sample, and the final image is reconstructed from a set of images taken at different grating positions. Here we demonstrate that with the help of a spatial light modulator, this technique can be used for imaging slowly moving structures in living cells.

Keywords Structured illumination microscopy · Live-cell imaging · Resolution improvement

Introduction

Fluorescence microscopy is an invaluable tool in the life sciences. In addition to imaging specifically labelled structures in fixed specimens, it allows us to study living organisms in a non-invasive and non-destructive manner. Unfortunately, the resolution is fundamentally limited by diffraction to about 200 nm in the lateral plane, whereas many sub-cellular structures are about an order of magnitude smaller. In the past decade, many new techniques have been developed to overcome this limitation, each with their advantages and shortfalls.

Recently developed techniques that rely on the localisation of single emitters (Betzig et al. 2006; Geisler et al. 2007; Hess et al. 2006; Lemmer et al. 2008; Lidke et al. 2005; Rust et al. 2006) can achieve lateral resolution down to 20 nm. The application of this technique to living cells has been demonstrated (Shroff et al. 2008), but at a frame acquisition time of 25–60 seconds, its use is limited to very slowly moving structures. Also, the determination of the axial position of the molecules is difficult, although 3D information can be obtained by introducing aberrations that give information about the axial position (Huang et al. 2008) or by a biplane imaging approach (Juette et al. 2008).

There are techniques for resolution improvement that are based on the depletion of unwanted fluorescence. Resolution below 50 nm (Donnert et al. 2006; Rittweger et al. 2009) can be achieved by stimulated emission depletion (STED) microscopy (Hell and Wichmann 1994; Schrader et al. 1995), where the resolution improvement is based on the use of a doughnut-shaped depletion beam around the centre of the excitation beam. Although not strictly necessary, these approaches are usually based on point-scanning to achieve the required intensity.

Another technique capable of improving the lateral and axial resolution in fluorescence microscopy is structured illumination microscopy (SIM), where a fine grating is projected onto the sample and the final high-resolution image is reconstructed from a set of images taken at different grating positions (Gustafsson 2000; Heintzmann and Cremer 1998). With this technique, resolution improvement by a factor of two can be achieved compared to

This article has been submitted as a contribution to the *Festschrift* entitled "Uncovering cellular sub-structures by light microscopy" in honour of Professor Cremer's 65th birthday.

L. M. Hirvonen · K. Wicker · R. Heintzmann (✉)
Randall Division of Cell and Molecular Biophysics,
King's College London, New Hunt's House,
Guy's Campus, London SE1 1UL, UK
e-mail: heintzmann@googlemail.com

O. Mandula
Faculty of Mathematics and Physics, Charles University,
Ke Karlovu 3, 121 16 Praha 2, Czech Republic

conventional wide-field fluorescence microscopy. As a wide-field technique, the data acquisition can be fast, and the final image can be reconstructed from nine frames of raw data to achieve nearly isotropic resolution improvement in the lateral plane. So far the application of this technique to biological imaging has been limited to fixed samples (Gustafsson 2000; Gustafsson et al. 2008), although an application to imaging living cells has been published while the current manuscript was under revision (Kner et al. 2009). Here we demonstrate that this technique is compatible with live-cell imaging. Although several images are required for the final image, slowly moving structures, such as mitochondria, can be imaged in living cells with structured illumination microscopy.

Materials and methods

Microscope

A custom-built wide-field microscope was used for imaging the samples. The basic set-up of the microscope is shown in Fig. 1. A 473-nm CW laser (M-Quadrat, Germany; 80 mW) was used for fluorescence excitation. A shutter (Vincent-D1, Uniblitz, NY) was used for controlling the on-time of the laser. The laser beam was focused with lens L1 ($f_1 = 25$ mm) through a 10-μm pinhole (Ph) and collimated with lens L2 ($f_2 = 500$ mm) to fill the screen of a spatial light modulator (SLM; HEO 1080 P, Holoeye Photonics, Germany), where computer-generated grating patterns were displayed. The diffracted orders were focused with lens L3 ($f_3 = 1{,}000$ mm), and lenses L4 ($f_4 = 150$ mm) and L5 ($f_5 = 200$ mm) were used for relaying the focused diffraction orders to the back focal plane of the objective (63 × NA1.2 water immersion, Leica, Germany). The objective was mounted on a piezo-controlled z-stage (P-725.2CD, Physik Instrumente, Germany). A $\lambda/2$ plate (Comar, UK) in a rotating stage (DRTM 40, Owis, Germany) was used for rotating the polarisation of the input beam so that the first orders were azimuthally polarised (perpendicular to the x and y components of the grating's k-vector) for maximum contrast of the grating within the sample. An additional polariser in a rotating stage (DRTM 40, Owis, Germany) was inserted after the $\lambda/2$ plate to clean up the polarisation. The fluorescence emanating from the sample was imaged through the emission dichromatic reflector DM (Comar, UK) and the emission filter via a tube lens (Leica, Germany; magnification 1.25×) to a cooled CCD camera (Imager Intense, LaVision, Germany; 12 bit, 1,376 × 1,040 pixels, 6.45-μm pixel size).

Sample preparation

The point-spread function (PSF) of the structured illumination microscope was measured using green fluorescent beads. The polystyrene beads (Duke Scientific, CA, USA), with a mean diameter of 71 nm (specified by the manufacturer), were diluted in ethanol. A drop of this solution was deposited on a coverslip and allowed to evaporate. The coverslip was mounted on a glass slide using deionised water as the mounting medium.

COS1 cells were used for biological imaging. The cells were cultured in Dulbecco's modified Eagle's medium (DMEM; Invitrogen, UK) containing 10% foetal bovine serum (Invitrogen, UK) and penicillin/streptomycin/glutamine (Invitrogen, UK), and plated on 22 × 22 mm #1.5 poly-L-lysine (Sigma, UK) coated glass coverslips at a density of 50K cells. The medium was changed to the same medium containing 100 nM MitoTracker Green FM (Invitrogen, UK) after 16–20 h and the cells were incubated at 37°C for 30 min. The cells were then washed with phosphate-buffered saline (PBS), and the coverslips were placed on glass slides for imaging, using PBS as the mounting medium.

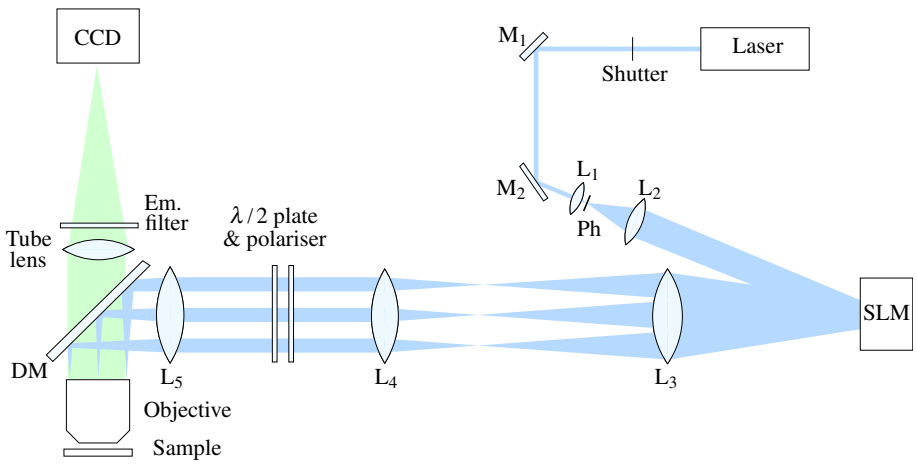

Fig. 1 A schematic diagram of the set-up for the structured illumination microscope

Data acquisition

The samples were illuminated with three diffracted orders, corresponding to five separated orders in the reconstruction process which was performed in 2D space. Four grating orientations were used, with five images per direction. The main period of the grating on the sample plane was 500 nm, with the 250-nm components present. The wide-field images were obtained by summing the images acquired with different grating phases and orientations. All imaging was done at room temperature.

Open-source software μManager (Amodaj and Stuurman 2006–2009; Stuurman et al. 2007) was used for controlling the microscope hardware. The data acquisition was automated using a Beanshell (Niemeyer 2008) script in μManager's scripting console.

Data reconstruction

Before image reconstruction in Fourier space, some pre-processing was performed in real space. First the background offset was subtracted using a 'dark' background image taken with the same integration time as the images but without illuminating the sample. The borders of the images were blended using a Hann window function with a flat central area to avoid artefacts arising from sharp edges. The images were corrected for drift using an iterative cross-correlation-based estimation for the drift (Pham et al. 2005). The images were also corrected for fluorescence intensity variations by adjusting the average intensity of each image to match the mean intensity of the image stack. The PSF used in the reconstruction process was an experimentally measured PSF (i.e. an image of a small bead).

The separation and the recombination of the frequency components was performed in Fourier space. Imperfections in the acquired data, such as imprecise shifting of the illumination pattern, bleaching of the pattern into the sample and fluctuations in the excitation intensity have a large influence on the quality of the separation of the frequency components. This was corrected computationally by optimising the separation matrix before the final unmixing of the components. The optimisation was performed iteratively by minimising the central value of the cross-correlations between two separated components before they are shifted.

The images were then resampled by zero padding in Fourier space to decrease the pixel size of the final image to accommodate increased resolution. The separated components were shifted with sub-pixel resolution for their true zero frequency to coincide with the centre peak. Where multiple components of the same frequency space region were present, they were averaged with frequency-dependent weights such that the signal-to-noise ratio was optimal and the goal function was achieved (Heintzmann 2003). The goal function was either a cosinusoidal or polynomial apodization function to avoid artefacts from the sharp edges of the new transfer function. A Wiener filter was also used to suppress noise amplification in the high frequencies. The final result was obtained by inverse Fourier transform (Mandula 2008).

Results

Measurement of PSF

To measure the PSF of the structured illumination microscope, the positions of 99 individual beads were recorded from the SIM image. A small region of interest (ROI) was extracted around each recorded position from both the SIM and the wide-field images. The beads were then centred with sub-pixel accuracy to the middle of the ROI and summed to obtain the experimental SIM and wide-field PSFs (Fig. 2b, c). A Gaussian curve was fitted to each of the summed images (Fig. 2a).

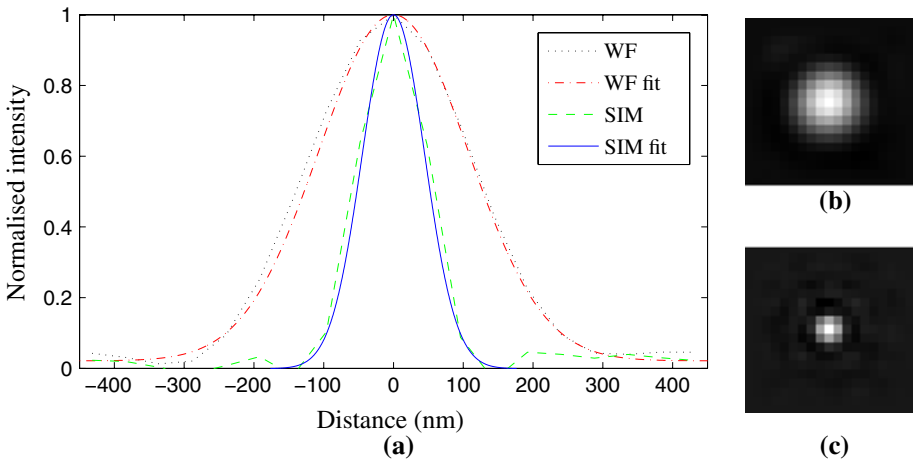

Fig. 2a–c Measurement of the PSF of the structured illumination microscope. **a** Cross-sections of the PSFs measured from an average of 99 beads with a mean diameter of 71 nm. A Gaussian fit to the averages gives a FWHM of 252 and 105 nm for the wide-field and structured illumination PSF (including the bead size, see text) respectively. **b**, **c** The sum of the beads in the wide-field and the structured illumination mode respectively. Pixel size: 48 nm

To account for the effect of the finite bead size on the PSF measurement, the bead was assumed to be a projection of a sphere along the axial direction (because the PSF is much more elongated in this direction). Its variance (σ^2) can be calculated along one of the other spatial directions (here x) as

$$\sigma^2 = \frac{r_{\text{bead}}^2 \int_{-1}^{1} \sqrt{1-x^2}x^2 \mathrm{d}x}{\int_{-1}^{1} \sqrt{1-x^2}\mathrm{d}x} = \frac{1}{4}r_{\text{bead}}^2 = \frac{1}{16}d_{\text{bead}}^2$$

where r_{bead} and d_{bead} are the radius and the diameter of the bead respectively. The full width at half maximum (FWHM) of the bead can be obtained from

$$\text{FWHM}_{\text{bead}} = 2\sqrt{2\ln 2}\,\sigma = \sqrt{\frac{\ln 2}{2}}d_{\text{bead}}$$

The FWHM of the PSF without the effect of the finite-sized bead can then be obtained from

$$\text{FWHM}_{\text{PSF}} = \sqrt{\text{FWHM}_{\text{meas}}^2 - \text{FWHM}_{\text{bead}}^2}$$

where $\text{FWHM}_{\text{meas}}$ is the FWHM of the image of the bead.

The measured FWHM of the wide-field bead image was 252 nm, corresponding to a PSF with a FWHM of 249 nm when taking into account the size of the beads. The FWHM of the reconstructed SIM bead image was 105 nm, corresponding to a PSF with a FWHM of 96 nm.

Imaging of a living cell

The data acquisition is fast enough to obtain images of living samples with slowly moving structures. Mitochondria are found in most eukaryotic cells, producing most of the cell's supply of chemical energy and playing an important role in the control of the cell cycle. Figure 3 shows a time series of mitochondria in a living Cos-cell, stained with MitoTracker Green. The images were acquired at 3-min intervals. Three orders were used for illumination, corresponding to five separated orders in the reconstruction, which also improves optical sectioning. Each structured illumination image was reconstructed from a total of 20 images with an image acquisition rate of about 1 image/second and 3 min between each high-resolution image. The movement of some of the mitochondria between the images can be clearly seen in Fig. 3i, j, which show an overlay of the first three images in the time series shown in red, green and blue respectively. As well as showing some details which cannot be seen in the wide-field images, the reconstructed structured illumination images clearly demonstrate improved optical sectioning.

Discussion

While the resolution improvement by linear structured illumination is limited to a maximum of a factor of two, no unusual properties are required from the fluorophores or the samples. Only three to five images are needed per direction, and three to four grating orientations are enough to obtain nearly isotropic resolution improvement in the lateral plane. The resolution improvement has been demonstrated on both fixed and living samples.

When illuminating with three orders it is possible to also improve the axial resolution with structured illumination microscopy. Even though such data can be processed in a slice-by-slice fashion (Mandula 2008), a true 3D processing

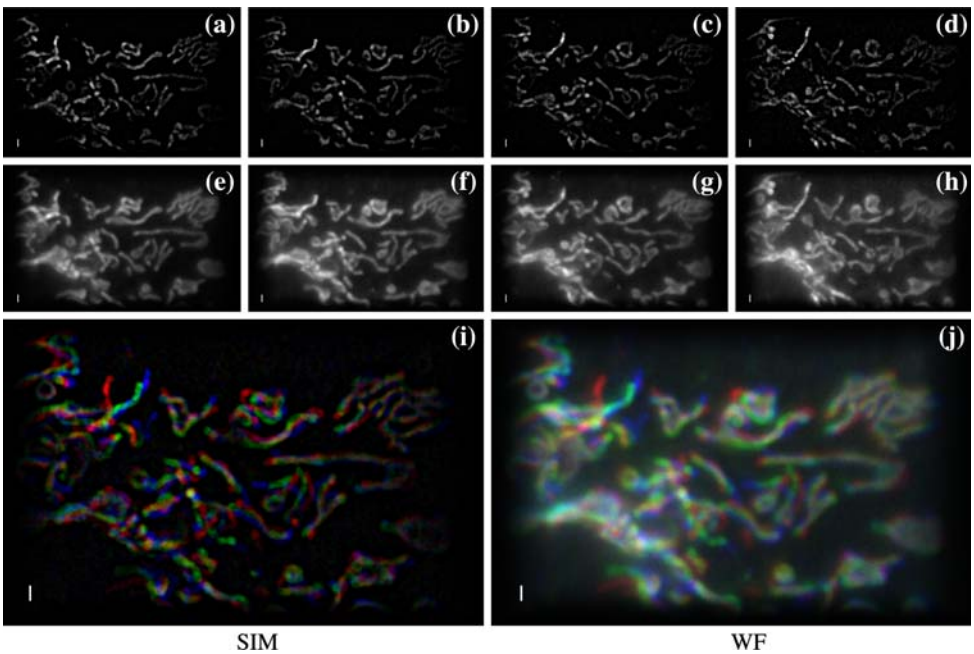

Fig. 3 A time series of mitochondria in a living Cos-cell stained with MitoTracker imaged with structured illumination microscopy (**a**–**d**) and wide-field equivalent (**e**–**h**), as reconstructed from the sum of the individual SIM images. The images were acquired at 3-min intervals. **i**, **j** Overlay of the first three images in the time series shown in *red*, *green* and *blue* respectively. *Scale bars* 1 μm

(Gustafsson et al. 2008) is advantageous. It is also possible to combine structured illumination with the I^5M technique (Shao et al. 2008) which, similar to standing wave (Bailey et al. 1993) or spatially modulated illumination microscopy (Failla et al. 2002), uses two opposing objective lenses to improve the axial resolution, yielding a resolution of about 100 nm in all three dimensions.

Further resolution improvement can be achieved with SIM if the linear relationship between the excitation and emitted intensity is broken (Heintzmann et al. 2002). Resolution below 50 nm has been demonstrated with fluorescent beads by saturating the excited state of the fluorophores, but in this case very high illumination intensity was needed (Gustafsson 2005). It could be possible to use recently discovered photoswitchable fluorophores (Ando et al. 2004; Bates et al. 2005; Heilemann et al. 2005; Lukyanov et al. 2000; Sabanayagam et al. 2005) to create the nonlinearity (Hirvonen et al. 2008). With these fluorophores the transition between the fluorescent and the dark state can be saturated instead of saturating transitions involved in the fluorescence excitation and emission. When the states are stable enough, these transitions are easily saturable, so no high intensity is needed, although very good photostability is required from the fluorophores.

Acknowledgments This work was funded by the Medical Research Council, Carl Zeiss MicroImaging GmbH and the International Agency for Atomic Energy.

References

Amodaj N, Stuurman N (2006–2009) μManager. http://micro-manager.org/

Ando R, Mizuno H, Miyawaki A (2004) Regulated fast nucleocytoplasmic shuttling observed by reversible protein highlighting. Science 306:1370–1373

Bailey B, Farkas DL, Taylor DL, Lanni F (1993) Enhancement of axial resolution in fluorescence microscopy by standing-wave excitation. Nature 366:44–48

Bates M, Blosser TR, Zhuang X (2005) Short-range spectroscopic ruler based on a single-molecule optical switch. Phys Rev Lett 94:101–108

Betzig E, Patterson GH, Sougrat R, Lindwasser OW, Olenych S, Bonifacino JS, Davidson MW, Lippincott-Schwartz J, Hess HF (2006) Imaging intracellular fluorescent proteins at nanometer resolution. Science 313:1642–1645

Donnert G, Keller J, Medda R, Andrei MA, Rizzoli SO, Lührmann R, Jahn R, Eggeling C, Hell SW (2006) Macromolecular-scale resolution in biological fluorescence microscopy. Proc Natl Acad Sci USA 103(31):11440–11445

Failla AV, Spoeri U, Albrecht B, Kroll A, Cremer C (2002) Nanosizing fluorescent objects by spatially modulated illumination microscopy. Appl Opt 41(34):7275–7283

Geisler C, Schönle A, von Middendorff C, Bock H, Eggeling C, Egner A, Hell SW (2007) Resolution of $\lambda/10$ in fluorescence microscopy using fast single molecule photo-switching. Appl Phys A 88:223–226

Gustafsson MGL (2000) Surpassing the lateral resolution limit by a factor of two using stuctured illumination microscopy. J Microsc 198:82–87

Gustafsson MGL (2005) Nonlinear structured-illumination microscopy: wide-field fluorescence imaging with theoretically unlimited resolution. Proc Natl Acad Sci USA 102(37):13081–13086

Gustafsson MGL, Shao L, Carlton PM, Wang CJR, Golubovskaya IN, Cande WZ, Agard DA, Sedat JW (2008) Three-dimensional resolution doubling in wide-field fluorescence microscopy by structured illumination. Biophys J 94:4957–4970

Heilemann M, Margeat E, Kasper R, Sauer M, Tinnefeld P (2005) Carbocyanine dyes as efficient reversible single-molecule optical switch. J Am Chem Soc 127:3801–3806

Heintzmann R (2003) Saturated patterned excitation microscopy with two-dimensional excitation patterns. Micron 34:283–291

Heintzmann R, Cremer C (1998) Laterally modulated excitation microscopy: improvement of resolution by using a diffraction grating. Proc SPIE 3568:185–195

Heintzmann R, Jovin TM, Cremer C (2002) Saturated patterned excitation microscopy—a concept for optical resolution improvement. J Opt Soc Am A 19(8):1599–1609

Hell SW, Wichmann J (1994) Breaking the diffraction resolution limit by stimulated emission: stimulated-emission-depletion fluorescence microscopy. Opt Lett 19:780–782

Hess ST, Girirajan TPK, Mason MD (2006) Ultra-high resolution imaging by fluorescence photoactivation localization microscopy. Biophys J 91:4258–4272

Hirvonen L, Mandula O, Wicker K, Heintzmann R (2008) Structured illumination microscopy using photoswitchable fluorescent proteins. Proc SPIE 6861:68610L

Huang B, Jones SA, Brandenburg B, Zhuang X (2008) Whole-cell 3D STORM reveals interactions between cellular structures with nanometer-scale resolution. Nat Methods 5(12):1047–1052

Juette MF, Gould TJ, Lessard MD, Mlodzianoski MJ, Nagpure BS, Bennett BT, Hess ST, Bewersdorf J (2008) Three-dimensional sub-100 nm resolution fluorescence microscopy of thick samples. Nat Methods 5(6):527–529

Kner P, Chhun BB, Griffis E, Winoto L, Gustafsson MGL (2009) Super-resolution video microscopy of live cells by structured illumination. Nat Methods 6(5):339–342

Lemmer P, Gunkel M, Baddeley D, Kaufmann R, Urich A, Weiland Y, Reymann J, Müller P, Hausmann M, Cremer C (2008) SPDM: light microscopy with single-molecule resolution at the nanoscale. Appl Phys B93:1–12

Lidke KA, Rieger B, Jovin TM, Heintzmann R (2005) Superresolution by localization of quantum dots using blinking statistics. Opt Exp 13(18):7052–7062

Lukyanov KA, Fradkov AF, Gurskaya NG, Matz MV, Labas YA, Savitsky AP, Markelov ML, Zaraisky AG, Zhao XN, Fang Y, Tan W, Lukyanov SA (2000) Natural animal coloration can be determined by a nonfluorescent green fluorescent protein homolog. J Biol Chem 275:25879–25882

Mandula O (2008) Patterned excitation microscopy. Master's Thesis, Charles University, Prague

Niemeyer P (2008) Beanshell. http://www.beanshell.org/

Pham TQ, Bezuijen M, van Vliet LJ, Schutte K, Luengo Hendriks CL (2005) Performance of optimal registration estimators. In: Rahman Z, Schowengerdt RA, Reichenbach SE (eds) Visual information processing XIV, Orlando, FL, USA. Proceedings of SPIE, vol. 5817, pp 133–144.

Rittweger E, Han KY, Irvine SE, Eggeling C, Hell SW (2009) STED microscopy reveals crystal colour centres with nanometric resolution. Nat Photonics 3:144–147

Rust MJ, Bates M, Zhuang X (2006) Sub-diffraction-limit imaging by stochastic optical reconstruction microscopy (STORM). Nat Methods 3(10):793–795

Sabanayagam CR, Eid JS, Meller A (2005) Long time scale blinking kinetics of cyanine fluorophores conjugated to DNA and its effect on Förster resonance energy transfer. J Chem Phys 123:224–708

Schrader M, Meinecke F, Bahlmann K, Kroug M, Cremer C, Soini E, Hell SW (1995) Monitoring the excited state of a fluorophore in a microscope by stimulated emission. Bioimaging 3:147–153

Shao L, Isaac B, Uzawa S, Agard DA, Sedat JW, Gustafsson MGL (2008) I^5S: wide-field light microscopy with 100-nm-scale resolution in three dimensions. Biophys J 94:4971–4983

Shroff H, Galbraith CG, Galbraith JA, Betzig E (2008) Live-cell photoactivated localization microscopy of nanoscale adhesion dynamics. Nat Methods 5(5):417–423

Stuurman N, Amodaj N, Vale R (2007) μManager: open source software for light microscope imaging. Microsc Today 15:42–43